15C.5

INTERACTION BETWEEN A MIDLATITUDE UPPER-LEVEL TROUGH AND TROPICAL CYCLONE DORA (2007) OVER THE SOUTHWEST INDIAN OCEAN

Marie-Dominique E. Leroux *

Laboratoire de l'Atmosphère et des Cyclones, unité mixte CNRS – Météo-France – Université de La Réunion, Sainte Clotilde, Reunion

1. INTRODUCTION

A question remains among the scientific community in the context of tropical cyclone (TC) intensity prediction: will an approaching upper-tropospheric synoptic-scale trough produce intensification or decay of a given TC?

Many observational studies and numerical modeling have documented TC-trough interaction. Hanley et al. (2001) introduced the "good trough/bad trough" terminology to sort troughs according to TC intensification. An approaching trough can have contradictory effects on the environmental ingredients that are crucial for TC intensification. On the one hand, it may induce significant vertical wind shear which is usually detrimental to TC intensity. On the other hand, it may increase upper-level divergence and enhance outflow poleward of the storm as well as import cyclonic eddy angular momentum (Molinari et al. 1995), all positive contributions to TC intensification. From a potential vorticity (PV) perspective, TC-trough interaction can be associated with PV advection from the trough toward the TC, which is beneficial below the level of the outflow anticyclone ("PV superposition principle", Molinari et al. 1998). The triggering of convection by upward velocities associated with the PV anomaly, as well as dry air intrusion from the low stratosphere, are other interesting processes that might have a role to play in TC-tough interactions.

Other studies (WMO 2010) have demonstrated that internal processes that modify the vortex structure such as an "eyewall replacement cycle" (ERC) are responsible for rapid intensity changes under favorable environmental conditions. The remaining work to get a comprehensive insight into TC-trough interaction is therefore to investigate the TC inner core during such interactions, and see whether external forcing can excite internal processes. For example, can a trough induce the development of a secondary wind maximum as suspected for Hurricane Elena by Molinari and Vollaro (1990)?

The present work is motivated by the fact that Rossby waves frequently break in the southwest Indian Ocean (Ndarana and Waugh 2011). High-PV anomalies, often associated with cutoff cyclones, form during the isentropic equatorward advection of stratospheric air into the troposphere and can be found at latitudes where TCs evolve and sometimes rapidly intensify.

Numerical experiments are conducted on TC Dora (2007) who rapidly intensified in the vicinity of an upper trough. We first describe vortex and PV interactions between the two cyclonic circulations associated with the TC and the approaching trough, before identifying the pathway to TC intensification under such upper-level forcing.

2. TC DORA AND THE MODEL

TC Dora rapidly intensified between 1800 UTC 31 January and 0000 UTC 3 February 2007 with a 50 hPa pressure fall from 975 hPa (Fig. 1, red lines). From late 1 to early 2 February, the intensification was temporarily slowed down by an ERC (Fig. 1, green lines), clearly identified on passive microwave imagery (not illustrated). When the maximum winds suddenly strengthened from 31 m s^{-1} to 43 m s^{-1} on the 1st of February, Dora was interacting closely with an upper-level PV anomaly on its southern side issued from Rossby wave breaking (Fig. 2). The PV anomaly was entrained toward and merged with the high cyclonic (negative) PV values associated with the TC circulation at mid-level (330 K, or about 400 hPa). The deepening of Dora occurred under hardly conducive conditions: ambient wind shear was large (above 9 m s^{-1} until 0600 UTC 02 February, reaching 12 m s^{-1}), and ocean heat content was below the 50 kJ cm^{-2} threshold that has been shown to promote high rates of intensity change.

Corresponding author address: Marie-Dominique Leroux, Météo-France DIRRE, Cellule Recherche Cyclones, BP4, 97491 Ste Clotilde, La Réunion.
E-mail: marie-dominique.leroux@meteo.fr

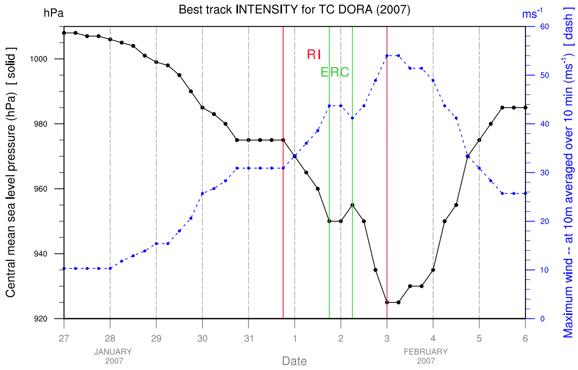

FIG. 1. Best track data for Dora (27 Jan-06 Feb 2007): central pressure (solid black line, left axis, hPa) and maximum wind speed (dashed blue line, right axis, $\mathrm{m\ s^{-1}}$).

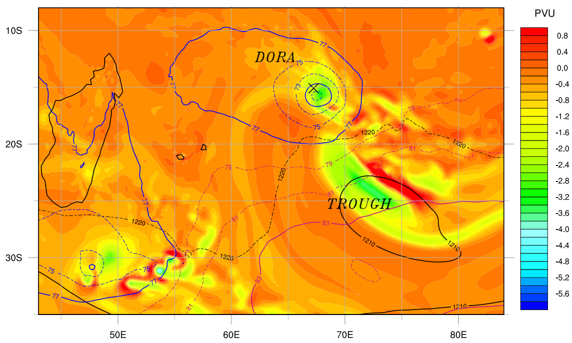

FIG. 2. Ertel potential vorticity on the 330 K isentropic surface (shading, in PVU $\equiv 10^{-6}\ \mathrm{m^2\ K\ s^{-1}\ kg^{-1}}$) for TC Dora at 0600 UTC 1 February 2007 in the ECMWF operational analysis at 0.25°-resolution. Contours are geopotential height at levels 925 hPa (blue and purple lines, mgp) and 200 hPa (black lines, mgp). The cross indicates Dora's best track center.

This makes Dora an interesting case to study RI in a "good trough" interaction context. Therefore, a 60-h forecast starting at 0600 UTC 31 January 2007 (12 hours prior to the onset of RI) is carried out using the limited-area model Aladin-Reunion in its 2011 operational version (hydrostatic, 70 vertical levels, 8-km horizontal resolution, Montroty et al. 2008). The domain extends from 0° to 32°S, and from 31.5° to 88.5°E. The forecast is initialized and coupled with the ECMWF global analyses, and Aladin's 3D-Var assimilation of cyclone wind bogus is used to get a realistic vortex structure at the basetime of the forecast. The simulation captures the PV interaction as well as the two periods of RI.

3. INTERACTION WITH PV ADVECTION

Tangential and radial winds are computed within a cylindrical framework following the storm center. Such a geometry highlights the asymmetric effects of the trough on the TC symmetric circulation. An anti-clockwise convention is used: convergent winds as well as tangential winds, relative and potential vorticity, are negative in a cyclonic circulation.

After 18-h integration, the approaching trough forces an asymmetric radial circulation across the storm with inflow in the south-southeastern sector, and outflow elsewhere, within the $400-200$ hPa layer, out to 1200 km (not illustrated). From 30 h to 37 h, unusual mean convergent flow can be found out to 250 km from the storm center at 200 hPa (Fig. 3a). The anticyclonic circulation initially present aloft Dora weakens as the trough enters the domain and moves toward the TC (Fig. 3b), leaving a cyclonic circulation at 200 hPa after 27h-integration. Cyclonic winds stronger than the storm winds between 26 and 33 hours materialize the trough and its associated jet streak located at 600 km away from the storm center (Fig. 3b, black line). The northwesterly winds of the jet enhance Dora's poleward outflow after 30 h at 200 hPa and increase upper-level divergence (not illustrated), which outbalances the detrimental effect of the strong vertical shear.

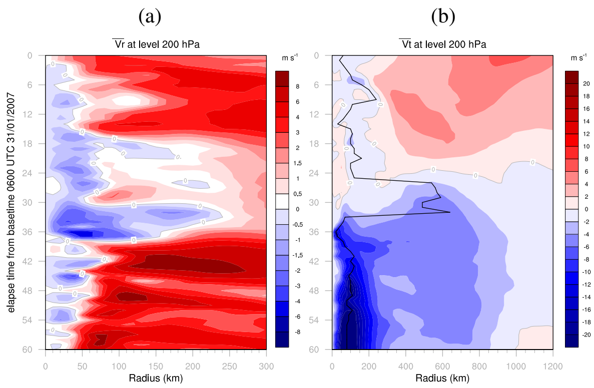

FIG. 3. Radius-time series of the 200 hPa azimuthally averaged (a) radial and (b) tangential velocity during the Aladin forecast of DORA. Radii go out to 300 km in (a) and 1200 km in (b). The black line in (b) indicates the radius where the cyclonic tangential wind are maximum.

This trough-induced flow enables PV advection from the trough directly into the TC core inside a 500-200 hPa layer. The PV intrusion has a strong downward vertical component giving a complex 3-dimensional advection. A first thin shallow intrusion brings negative PV values into the TC core from 26 to 37 hours (labeled "A" in Fig. 4a). The second and major PV advection is associated with the main tropopause folding and goes as deep as 500 hPa (labeled "B" in Figs. 4a and b). While the high-

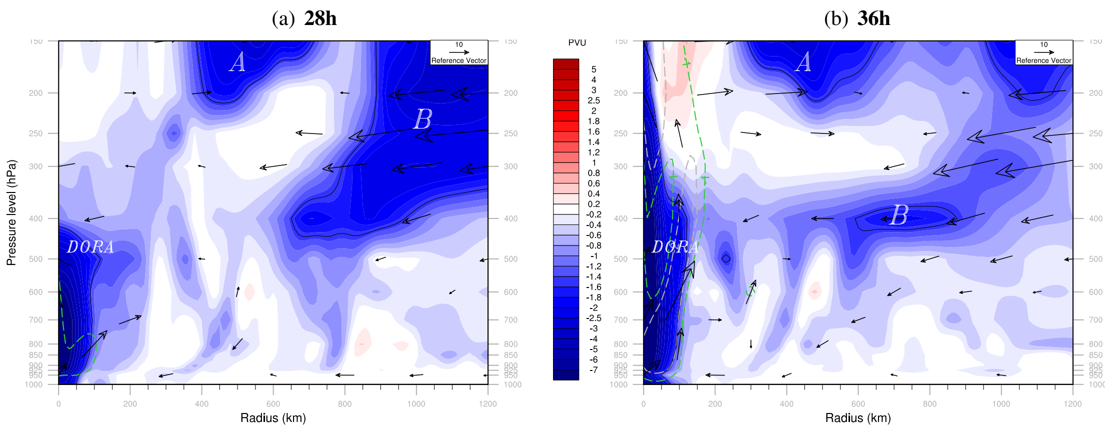

FIG. 4. Vertical cross sections of the PV (shaded, with the -1.5 PVU contour blackened) from the TC center to the south-southeast after (a) 28h- and (b) 36h-integration. Arrows show radial and vertical (-10*omega) velocity above 5 m s^{-1}(reference arrow indicated in legend). Dashed green (gray) contours indicate the regions were omega is less than -1. (-2) Pa s^{-1}.

est PV quantity associated with the main trough at upper levels (250-150 hPa) does not progress much further and stays outer than 400 km, the PV distribution stretches underneath toward the storm center (compare Figs. 4a and b). A small negative PV anomaly detaches at mid-levels and feeds the core with cyclonic PV from 33 h to 40 h (Fig. 4b). Once the storm cyclonic circulation spins up (after 37 h at upper levels, 40 h at mid-levels), divergent flow prevents PV advection into the TC core and negative PV values spiral at the outskirts. The trough then rapidly goes away.

Although PV is advected downshear away from the TC core too, a PV budget over a 300-km radius cylinder representing the storm confirms that the total lateral PV flux decreases with time towards more negative values until about 36 h, as the PV tendency.

4. A PATHWAY TO INTENSIFICATION

Such environmental PV distribution may intensify the TC through eddy fluxes of both angular momentum and potential vorticity (Molinari et al. 1995, 1998). They are evaluated by computing Eliassen-Palm (EP) fluxes in a cylindrical and isentropic framework following Molinari et al. (1995). EP flux diagrams (Fig. 5) show that the trough imports cyclonic eddy angular momentum fluxes (inward arrows with negative EP divergence in blue contours) at upper- to mid-levels. Fluxes penetrate inside a 400-km annulus after 24 h. They produce increasing cyclonic mean tangential wind and can explain the decay of the mean outflow anticyclone. The trough signature suffers vertical splitting as previously seen (PV field, Fig. 4b). From 36 to 40 h, cyclonic forcing is located outside the eyewall at about 100 km (blue contours in Fig. 5) while weakening is evident around the eyewall at 50 km (red contours). This cyclonic spinup extends through the entire troposphere which is original in the literature. The evolution of the radius of maximum winds at 850 hPa confirms the characteristic signature of an ERC (Willoughby et al. 1982). A first small intensification period occurs between 32 h and 34 h while the inner eyewall contracts (40 km). An outer wind maxima then develops between 36 h and 40 h (80 km). Contraction of this outer eyewall is associated with a period of rapid intensification (40-44 h). The development of the outer wind maximum as well as the shift of maximum upward velocities toward outer radii is also visible at mid-levels (not illustrated).

The adiabatic approximation used for calculating the EP fluxes could question the interpretation of such diagnostics in the TC inner-core where diabatic processes are involved. Therefore, a tangential wind budget is computed in pressure and cylindrical coordinates following Persing et al. (2002). The wind starts to increase at the periphery of the TC after 29 h (Fig. 6, right upper panel) in correlation with eddy momentum source throughout the troposphere at such radii (not illustrated but as in the EP flux diagram in Fig. 5 although around 200 km). The close proximity of the trough is evident at 36 h: vorticity fluxes by the mean flow (MVF) and by the eddies (EVF) both enhance the cyclonic circulation at upper to mid-levels where convergence appears (blue contours and dotted lines in Fig. 6, lower panels). Vertical advection of the tangential wind by the mean environmental upward motion forced by the upper tropospheric trough is also responsible for cyclonic spin up within the outer eyewall after 36 h (when convective updrafts start tilting outwards). As the trough departs (after 42 h), the TC becomes vertically stacked again. At 42 h, the outer eyewall has substituted for the main eyewall and has already contracted to 50 km (not illustrated).

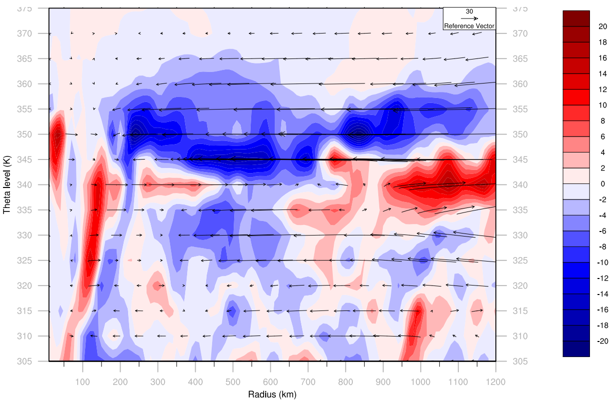

FIG. 5. Radius-theta cross section of EP flux vectors and their divergence (shaded) after 38h-integration. The divergence contour interval is 10^4 Pa m^2 K^{-1} s^{-2}; horizontal and vertical arrow scales are 1.3×10^8 Pa m^3 K^{-1} s^{-2} and 9.3×10^2 Pa m^2 s^{-2} (reference indicated in legend).

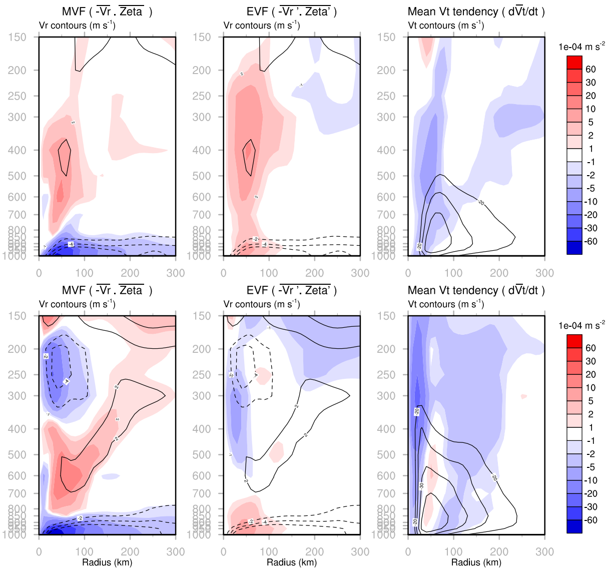

FIG. 6. Vertical cross sections of the mean (MVF) and eddy (EVF) vorticity flux terms in the tangential wind budget equation, as well as the tangential wind tendency (right panel), after 29h- (top) and 36h- (bottom) integration. Shading contours are indicated in the legendbar. The contours superimposed are mean radial velocity (MVF and EVF panels) and tangential wind (right plot).

5. CONCLUSION

Diagnostics show that Rossby-wave breaking of the trough on Dora's initial upper-level anticyclone deforms the PV anomaly which tilts towards the equator at mid-levels and advects negative PV values into the TC-core between 24 and 40 hours at mid and upper-levels. Eddy angular momentum forcing associated with the approaching trough is responsible for the decay of the upper-level anticyclone and the cyclonic spin up of the TC through the whole troposphere, which reduces vertical shear over the storm and can favor greater intensification rate (positive feedback). EP flux diagnostics and tangential wind budgets show that the trough forces an ERC between 36 and 42 h, therefore explaining the pathway to storm intensification under upper-level forcing, and confirming the suspicions of Molinari and Vollaro (1990). The ERC was observed for Dora around the same time than in the simulation suggesting that it is not an artefact from the Aladin model and that it can be simulated by a moderate resolution hydrostatic model which does not resolve convective processes (at least when the ERC is induced by external forcing). Future PV surgery experiments will modify the initial characteristics of the trough and see if (and how) the intensification is modified.

REFERENCES

Hanley, D., J. Molinari, and D. Keyser, 2001: A compositive study of the interactions between tropical cyclones and upper-tropospheric troughs. *Mon. Wea. Rev.*, **129**, 2570–2584.

Molinari, J., S. Skubis, and D. Vollaro, 1995: External influences on hurricane intensity. Part III: potential vorticity structure. *J. Atmos. Sci.*, **52**, 3593–3606.

Molinari, J. and D. Vollaro, 1990: External Influences on Hurricane Intensity. Part II: Vertical Structure and Response of the Hurricane Vortex. *J. Atmos. Sci.*, **47**, 1902–1918.

Molinari, J., D. Vollaro, F. Alsheimer, and H. E. Willoughby, 1998: Potential vorticity analysis of tropical cyclone intensification. *J. Atmos. Sci.*, **55**, 2632–2644.

Montroty, R., F. Rabier, S. Westrelin, G. Faure, and N. Viltard, 2008: Impact of wind bogus and cloud- and rain- affected SSM/I data on tropical cyclone analyses and forecasts. *Quart. J. Roy. Meteor. Soc.*, **134**, 1673–1699.

Ndarana, T. and D. W. Waugh, 2011: A Climatology of Rossby Wave Breaking on the Southern Hemisphere Tropopause. *J. Atmos. Sci.*, **68**, 798–811.

Persing, J., M. T. Montgomery, and R. E. Tuleya, 2002: Environmental Interactions in the GFDL Hurricane Model for Hurricane Opal. *Mon. Wea. Rev.*, **130**, 298–317.

Willoughby, H. E., J. A. Clos, and M. G. Shoreibah, 1982: Concentric eyewalls, secondary wind maxima, and the evolution of the hurricane vortex. *J. Atmos. Sci.*, **39**, 395–411.

WMO, 2010: Workshop topic reports for Tropical Cyclone Structure and Intensity Change. *Seventh WMO International Workshop on Tropical Cyclones*, World Meteorological Organisation.